

CONTROL AND ENERGY MANAGEMENT SCHEME FOR A PV/SC/BATTERY HYBRID RENEWABLE POWER SYSTEM

Syed Zulqadar Hassan^{*1}, Hui Li¹, Tariq Kamal², Sidra Mumtaz³, Laiq Khan³, Irfan Ullah¹

¹State Key Laboratory of Power Transmission Equipment and System Security and New Technology, School of Electrical Engineering, Chongqing University, Chongqing, China

²Department of Electrical and Electronics Engineering, Sakarya University, Faculty of Technology, Serdivan/Sakarya, Turkey

³Electrical Engineering Department, COMSATS Institute of IT Abbottabad, Pakistan

cqulh@163.com, tariq.kamal.pk@ieee.org, sidramumtaz@ciit.net.pk, laiq@ciit.net.pk, irfan.ee@cqu.edu.cn

Correspondencing author: syedzulqadar.hassan.pk@ieee.org.

ABSTRACT: *This study describes modeling, controlling and energy management of a Hybrid Renewable Power System (HRPS). It provides a Photovoltaic (PV) array as a primary energy source and an energy storage system based on Supercapacitor (SC) and battery bank. The PV, SC and battery are connected to a common DC bus through three controlled non-isolated DC–DC converters. The complete architecture is synchronized to the utility grid via three phase hysteresis current controlled inverter to improve the overall reliability of the system. A classically-based control scheme is proposed which decides the power that must be generated by the PV and/or stored in the SC or the battery storage system, considering the available power, the power required by the utility grid and the State-of-Charge (SOC) of the SC and battery. The dynamic performance of the proposed system is tested under real record of weather patterns and load conditions for a small community at Chongqing, China. Matlab/Simulink results are provided to test the effectiveness of the proposed system in terms of power transfer, load sharing, stability and power quality.*

Keywords: Hybrid Renewable Power System, Energy management, PV system, Storage system, System stability & Power quality analysis

INTRODUCTION

Growing environmental concerns, continuous increase in energy demand all over the world, depletion of conventional energy resources and recent development in power electronics, have opened the door for more power generation from Renewable Energy Sources (RESs) [1]. Nevertheless, these RESs have experienced certain major problems such as deregulation when they are used without backup system. For instance, a PV system would not provide perfect services to the grid or load during cloudy weather or at night time. Natural variations in weather pattern can create power oscillations in a PV system. In addition, the power supplied by a PV system is difficult to store [2]. The effective way to remove these obstacles is to design a HRPS with a smart power management strategy.

A HRPS removes the drawback of a single RES by taking the best possible use of each individual energy source and storage device [3]. The best possible solution for energy storage is a SC or battery, which provides the benefits of high efficiency and quick output response. The power density of the SC and the energy density of batteries are very high; and both have very fast instantaneous response [4, 5]. Therefore, these can offer better transient stability during sudden variation in demand and solar radiation. Since, utilization of SC and battery with PV can provide the most suitable effective hybrid topology.

Several hybrid systems containing PV with storage devices have been proposed in the past. In [6], a PV/battery system for a grid-off applications has been developed. A hybrid system based on PV with hydrogen energy (fuel cell) and battery has been suggested in [7]. The advantages of PV with a battery system in terms of electricity cost and customer satisfaction at demand side have been explored in it [8]. The application of SC/battery in PV based system has been designed in [9]. The role of SC in the PV system has been studied in [10]. In [11, 12], coordinated control and energy management of PV/SC/battery hybrid systems have been discussed. Similarly,

in [13] the authors performed study on the effect of SC in a standalone off-grid PV system has concluded that an addition of SC significantly improves the performance of a battery based PV system. Management and conversion of wind energy to hydrogen and battery is developed in [14]. In [15], the author simulated a PV/wind/SC/battery for grid-independent applications. The designing of PV/FC/wind hybrid system for proper energy management is presented in [16]. The unit sizing and control of HRPS is designed in [17]. In [18], the authors described a cost effective power generation using renewable energy sources. The common drawback of the above mentioned systems consider constant climatological variables, while some of the authors supported their proposed work considering the virtual made weather patterns.

This paper provides modeling, control and classical based energy management strategy combining PV array, SC module, battery bank and a set of loads for grid-off and grid-on applications while taking solar irradiance levels, temperature and loads for a summer day at Shapingba Chongqing, China. The proposed energy management system is simple and based on a classical switching logic algorithm. The proposed algorithm generates the dynamic references for each subsystem and effectively utilized all the energy sources and storage system according to different weather patterns and load conditions. The proposed system and algorithm confirms 24 H power flow with better reliability and power quality.

This study is organized in numbers of sections. Section 2 provides the system description. The control of different components have been given in Section 3. Section 4 focused on the system modeling. Section 5 provided the proposed energy management algorithm. Simulation results have been given in Section 6. Section 7 concluded the paper.

SYSTEM DESCRIPTION

There are two buses i.e., DC and AC bus in the proposed PV/SC/battery HRPS. PV, SC and battery build the assembly of DC bus, and the transferring of power happens among these

components through a classical based energy management system. AC bus connects residential load and utility grid to the proposed system. The output voltage of PV is adjusted through DC–DC boost converter while the power flow of SC and battery with the system happen through two non-isolated buck boost converters.

The DC bus supplies power to the grid and grid-connected load using three phase inverter. It is essential to state that the

HRPS is flexible and can extend as a new PV, SC or battery are attached to the existing ones without growing the circuit complexity. The performance and stability of the proposed system needs the simulation over a period of time. Therefore, for each distinct component steady-state simulation models have been followed. Figure 1 defines the schematic layout of the HRPS.

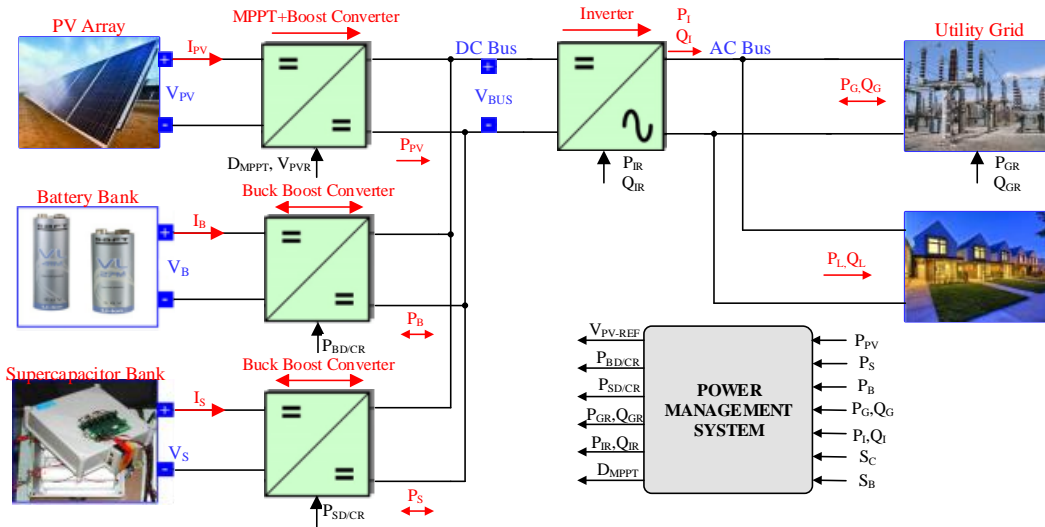


Figure 1: Schematic layout of the proposed HRPS

CONTROL OF SYSTEM COMPONENTS

Control of Photovoltaic System

The conversion efficiency of light energy into electrical energy is very low for PV systems. Since, it is required to fully convert the available light energy into electrical energy. For this purpose, the PV system is operating at Maximum Power Point (MPP). MPP is the ideal point at which PV system generates its maximum/rated power. To perform maximum power transfer, an Incremental Conductance Algorithm (ICA) based Maximum Power Point Tracking (MPPT) is incorporated in boost converter. The controller used for controlling PV system is Proportional Integral Derivative (PID) controller. The error “e” signal is generated by ICA. The PID tries to minimize the error signal by generating appropriate duty cycle. The entire control scheme is depicted in figure 2.

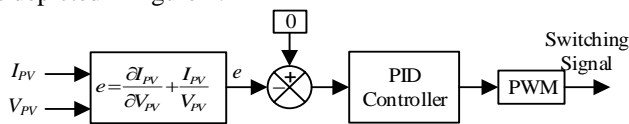


Figure 2: Control schematic of PV system

Control of Battery

A battery is a static storage device and needs proper voltage level for charging/discharging purpose. Stepping up/down operation of voltage level is achieved by coupling buck-boost converter with battery as illustrated in figure 1. The reference power for buck-boost converter is generated by Power Management System (PMS). Using reference power, reference current (I_i) is calculated i.e., $I_i = P_{BD/CR} / V_B$. Based

on I_i , the switching operation (i.e., buck or boost) is determined. The control scheme of a battery system is shown in figure 3.

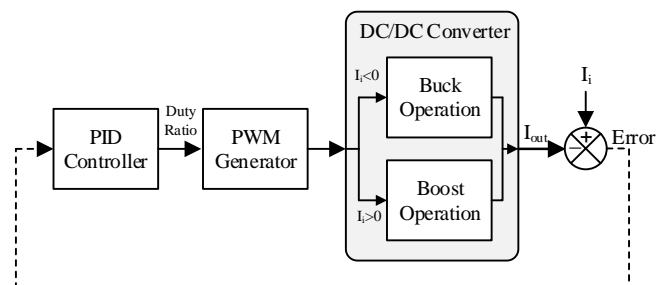


Figure 3: Control diagram of SC/Battery system

Control of Super-capacitor

The SC is also a static energy storage device with high power density. Therefore, it is directly coupled to DC bus with corresponding DC-DC converter as shown in figure 1. The DC-DC converter performs two operations i.e., firstly, it steps up/down the voltage level for charging/discharging purposes and secondly it regulates the DC bus. The reference current (I_i) is calculated using $P_{SD/CR}$ and given as $I_i = P_{SD/CR} / V_{SC}$. PID controller tries to equate the output current to reference current while PMS controls the operation of converters (i.e., buck or boost) based on I_i as shown in figure 3.

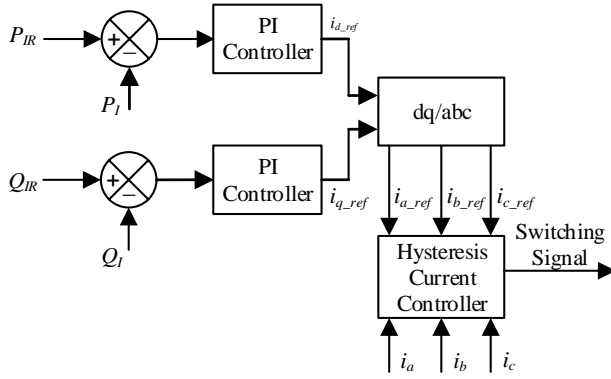


Figure 4: Control system of grid connected inverter

Control of Grid Connected Inverter

The output of DC is coupled to the grid via unidirectional IGBTs based three phase inverter. The inverter is controlled via Proportional Integral (PI) controllers followed by hysteresis current control method as presented in figure 4. The proposed control scheme provides proper pulses for driving the controllable switches of the inverter. The purpose of PI controller is to measure the errors between the reference and actual values of the reactive and real powers. Since, The PI controllers work is to reduce or eliminate the error. Based on error, the PI generates the corresponding dq-references. Using dq/abc transformation, current in-terms of abc reference is generated. After taking the difference with actual currents, it passes through hysteresis comparator and it generates the corresponding signals for inverter switches.

SYSTEM MODELING

Photovoltaic Array Modeling

Initially, a solar cell is made from silicon crystal which comprises of semiconductor material layers. It is observed that the solar arrays are then made from solar cells using different combinations of parallel and series, sequences depending upon available size and power required. There are different types of equivalent circuit models are presented for PV module [19]. Among these, a well-known model is single diode, which has a shunt (R_{sh}) and series (R_s) resistances [20], shown in figure 5. I_{ph} is the current produced by PV which is related to solar irradiation (λ) using 4.

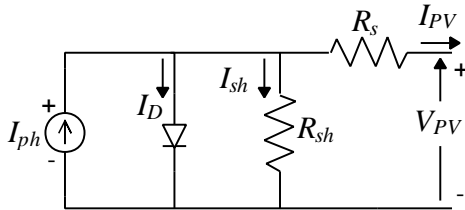


Figure 5: PV single diode model

The series and shunt resistances represent internal resistance and leakage current [21]. The PV cell current can be written as follows:

$$I_{PV} = I_{ph} - I_D - \frac{V_D}{R_{sh}} \quad (1)$$

where the diode current (I_D), diode voltage (V_D) and photo-current (I_{ph}) are expressed by:

$$I_D = I_0 (e^{V_D/V_T} - 1) \quad (2)$$

$$V_D = (V_{PV} + I_{PV} R_s) \quad (3)$$

$$I_{ph} = (I_{SC} + A(T - T_{ref})) \lambda \quad (4)$$

The variables are defined in appendix A. Voltage-current (V-I) characteristic of a PV can be given by:

$$V_{PV} = N_s \left(\frac{AkT}{q} \right) \ln \left\{ \frac{N_p I_{ph} - I_{PV} + N_p I_0}{N_p I_0} \right\} - \frac{N_s}{N_p} I_{PV} R_s \quad (5)$$

Battery Modeling

The battery can be modeled in different ways, but in this research, it is modeled with two RC circuits connected with each other in series combination as shown in Figure 6. The open circuit voltage (V_{oc}) and internal resistance (R_1) are related to the state of charge of the battery (S_B) using (6). The voltages across the two capacitors (e_1 , e_2) and S_B are the three state variables for the battery [22].

$$V_{oc} = 338.8 \times [0.94246 + 0.05754 \times S_B] \quad (6)$$

$$R_1 C_1 \frac{de_1}{dt} + \left(\frac{R_1 + R_2}{R_2} \right) \cdot e_1 = V_{oc} + \frac{R_1}{R_2} \cdot e_2 \quad (7)$$

$$R_b C_2 \frac{de_2}{dt} + e_2 = e_1 - R_2 I_t \quad (8)$$

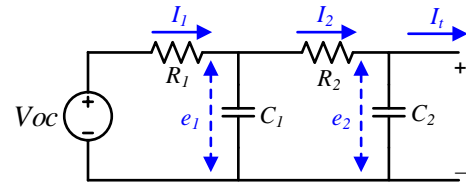


Figure 6: Electrical model of battery system

The third state variable of the battery system is S_B and defined as:

$$\frac{dB_{SOC}}{dt} = \frac{I_t}{Q_{max}} \quad (9)$$

where Q_{max} is the maximum battery charge (Ah). After solving above equation, the battery current can be written as:

$$I_t = \frac{V_{oc} - \sqrt{V_{oc}^2 - 4(R_1 + R_2)P_{out}}}{2(R_1 + R_2)} \quad (10)$$

where P_{out} is the output power of battery (W).

Super-capacitor Modeling

In this research work, classical model of SC [2], is used which consists of double layer capacitance, an equivalent series and an equivalent parallel resistances as shown in figure 7. The complete nomenclature used for modeling SC is given in Table 1.

Table 1: Nomenclature of SC

Symbol	Description
C	Capacitance (F)
R_p, R_s	Equivalent parallel and series resistance
C_t, R_t	Total capacitance and resistance of SC
V_{ini}, V_{final}	Initial and Final voltage of SC (V)
n_p	No of total parallel string
n_s	No of series capacitors connected in each string
E_{SC}	Energy drawn or absorbed by SC

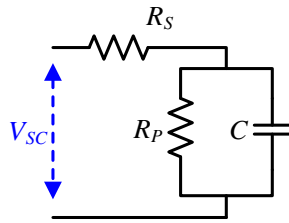


Figure 7: Electrical model of SC

The series and parallel resistance represents the charging/discharging and loss resistances, respectively. The parallel resistance only affects the long term storage of SC. The energy drawn from SC has a direct relation with voltage [23], given by:

$$E_{SC} = \frac{1}{2} C (V_{ini}^2 - V_{final}^2) \tag{11}$$

When SC supplies power, its voltage start decreasing slowly using (11) and start increasing when it stores energy. Usually, SC is used for heavy duty loads, they can satisfy the load demand by combining different units in the series or parallel combinations. The terminal voltage can be obtained by the number of series cells connected in one branch, while the total capacitance of SC is calculated by the number cells connected in parallel. The total resistance and capacitance can be given by:

$$R_t = n_s \frac{R_s}{n_p} \tag{12}$$

$$C_t = n_p \frac{C}{n_s} \tag{13}$$

ENERGY MANAGEMENT SYSTEM OF PROPOSED HRPS

A 261 kW PV system is used in this study is to supply power at best radiation and temperature. The battery bank and SC module are operated in parallel with PV. The function of the SC module and battery bank are to store the excess power from DC bus and then deliver it back in case when needed. In addition, the mismatches and load tracking problems of PV are compensated by SC module and battery.

A control scheme is developed to track the demands during daytime and after sunset by using the PV/SC/battery HRPS as shown in the figure 8. The classical based switching

algorithm controls the whole energy measurement. Based upon the required inputs listed in table 2, the proposed energy management system generates the command signals for the power converters attached to the inputs/outputs of the components used in the HRPS.

Table 2: Inputs/Outputs of proposed PMS

Symbol	Description
P_L	Residential Load Power
P_G	Grid Power
P_B	Battery Power
P_S	Super-capacitor Power
P_{PV}	PV Power
S_B	SOC of Battery
S_S	SOC of Super-capacitor
P_{BDR}	Battery Discharging Reference Power
P_{BCR}	Battery Charging Reference Power
P_{SDR}	Super-capacitor Discharging Reference Power
P_{SCR}	Super-capacitor Charging Reference Power
P_{GR}	Grid Reference Power

The operating strategies employed in the power management system are based on certain algorithm. This algorithm is described below.

Generalized Algorithm

1. All parameters are observed, i.e., $P_{PV}, P_G, P_L, P_B, P_S, S_B$ and S_S .
2. Check the condition $P_L = P_{PV} \pm P_G \pm P_S \pm P_B$, if it is true, then goto 1, otherwise goto next step.
3. Check the condition $P_L > P_{PV}$, if it is true, then goto next step else goto step 9.
4. Check $T_B > 20\%$, if true, then discharge the battery and goto next step else goto 6.
5. Check the condition $P_L - P_{PV} - P_B > 0$, if true, then goto next step, otherwise goto 1.
6. Check $T_S > 20\%$, if true, then discharge SC and goto next step else goto 8.
7. Check the condition $P_L - P_{PV} - P_B - P_S > 0$, if true, then goto next step, otherwise goto 1.
8. Apply all the remaining deficient power reference to grid. As the power density of SC is very high, so it is capable of providing power and goto 1.
9. Check $T_B > 90\%$, if false, then charge the battery and goto next step else goto 11.
10. Check the condition $P_L - P_{PV} - P_B < 0$, if true, then goto next step, otherwise goto 1.
11. Check $T_S > 90\%$, if false, then charge the SC and goto next step else goto 13.
12. Check the condition $P_L - P_{PV} - P_B - P_S < 0$, if true, then goto next step, otherwise goto 1.
13. Deliver all the remaining excess power to the grid and goto 1.

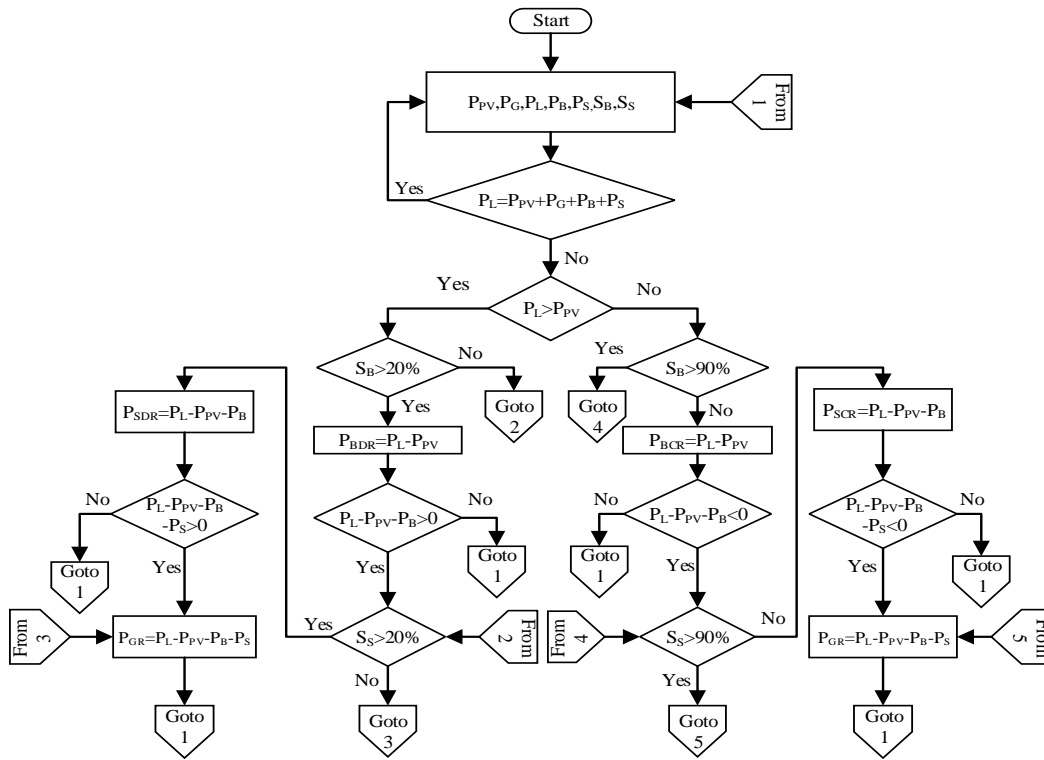


Figure 8: Flow chart of proposed algorithm

SIMULATION RESULTS AND DISSCUSION

Weather Data

The weather patterns followed in this HRPS are ambient temperature (°C) and solar irradiance (W/m²). The temperature is collected hourly basis while solar irradiance is taken at the interval of one hour. In this research the irradiance and temperature are taken from different weather channels. The weather data used in this research are of a typical summer day dated 13 June 2015 at Chongqing as presented in figure 9.

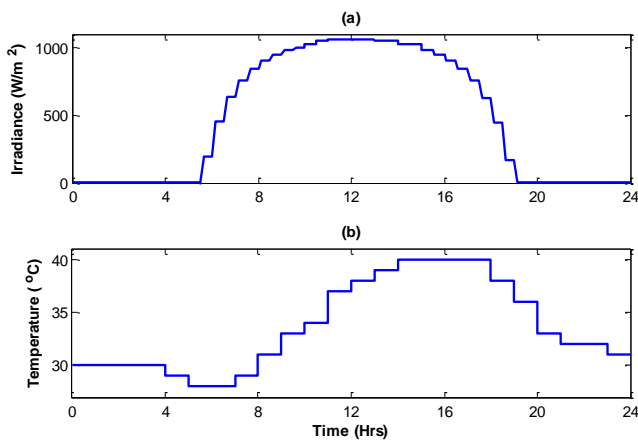


Figure 9: Weather statistics (a) Irradiance (b) Temperature

load and average load are calculated as 2.8 kW and 2.02 kW per home. The peak load starts from 18 H and ends at 21 H. The residential load demand of 100 houses located at Chongqing, China is considered. The power factor is taken as 0.8 during simulation. On the basis of power factor, the reactive powers of residential load, grid and inverter is calculated. The positive means grid is supplying power while negative means grid is taking power and zero means grid is disconnected from the proposed HRPS. Residential load real and reactive power is shown in figure 10. Grid real and reactive power is shown in figure 11 whereas the real and reactive power of main inverter is shown in figure 12.

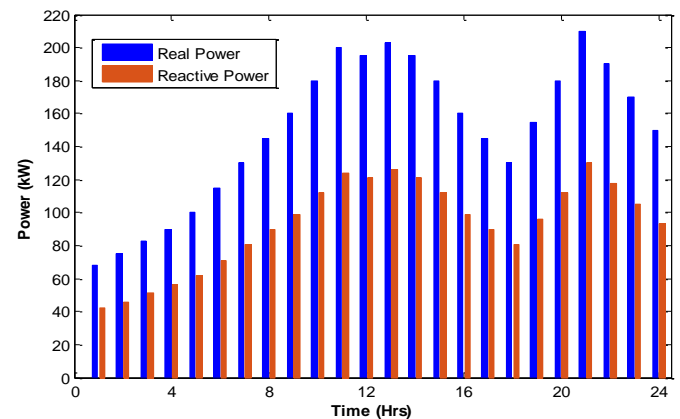


Figure 10: Residential load power demand

Dynamic Load

The proposed HRPS can be used for grid-on and grid-off applications. The HRPS provides power to residential load. The fixed power is determined by inflexible loads like ceiling fan, air conditions, refrigerators etc. For lighting load, the power consumption is calculated using averaging. The peak

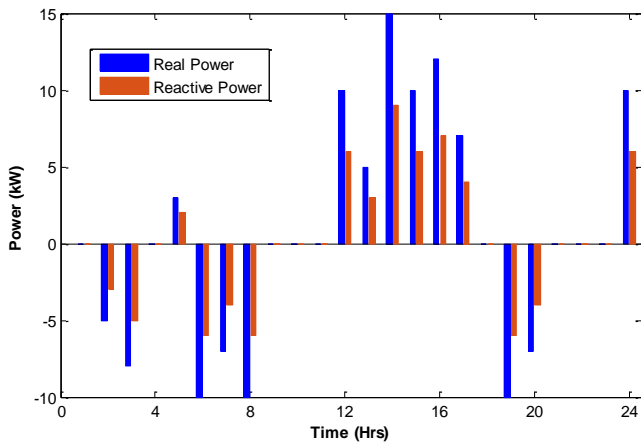


Figure 11: Utility grid power demand

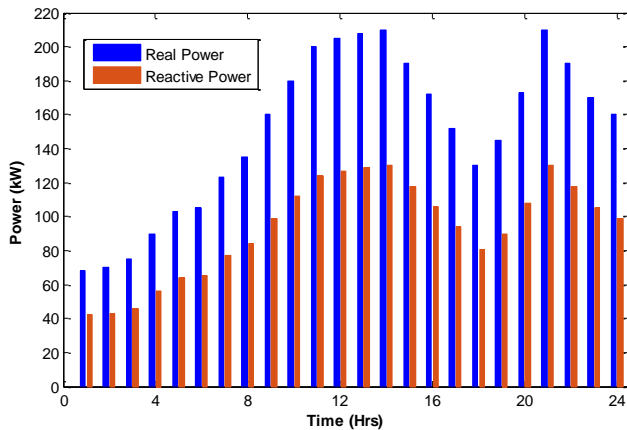


Figure 12: Power flow through main inverter

Residential Load Results

The residential load demand is shown in figure 13. In figure 13, the solid blue lines show the actual power delivered to the load while the dotted red line represents the load demand reference. The entire simulation is carried out for 24 H. At $t=0$ to 10 H, the load demand increases from 67 kW to 200 kW of real power while 40 kW to 120 kW of reactive power. There are two peaks presented in the figure 13. The first peak lies at 12 H while the second peak lies at 21 H. The first peak is due to the office timing and peak sun hours while the second peak is due to the night timing which includes the lighting and cooling loads. The off peak hours are 0-6 H, it is due to night timing. However, the residential load demand varies between 50 kW and 210 kW.

Utility Grid Results

Figure 14 shows the real and reactive actual and reference powers of the utility grid. Generally, the grid is used to take power during peak load hours while it delivers powers during off peak load hours. During 0 to 8 H, it is off peak hours and the grid is supplying power ranging from 1 to 10 kW. Furthermore, during peak load hours i.e., 11 to 17 H, the grid takes power from HRPS ranging from 1 to 15 kW. Similarly, the corresponding reactive power is provided or delivered. The reference power shown in figure 14 is a step change while in actual scenario, the PI based controller is used to control the grid power, hence, an overshoots, undershoots, transients and settling time are the major factors behind a

slow response with respect to step change. All the above parameters can be clearly observed from the figure 14.

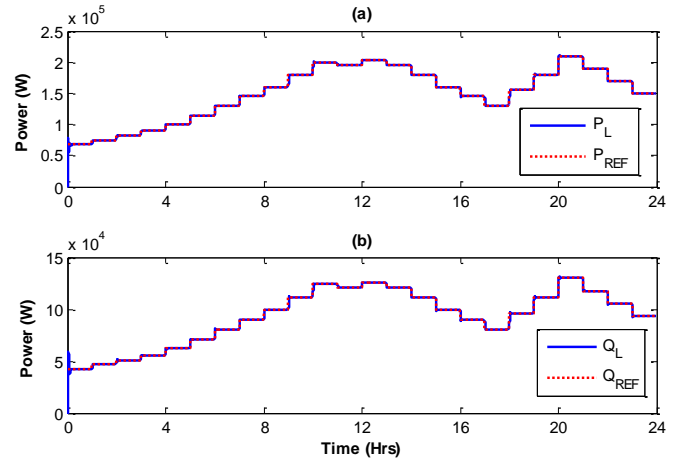


Figure 13: Residential load (a) Real power (b) Reactive power

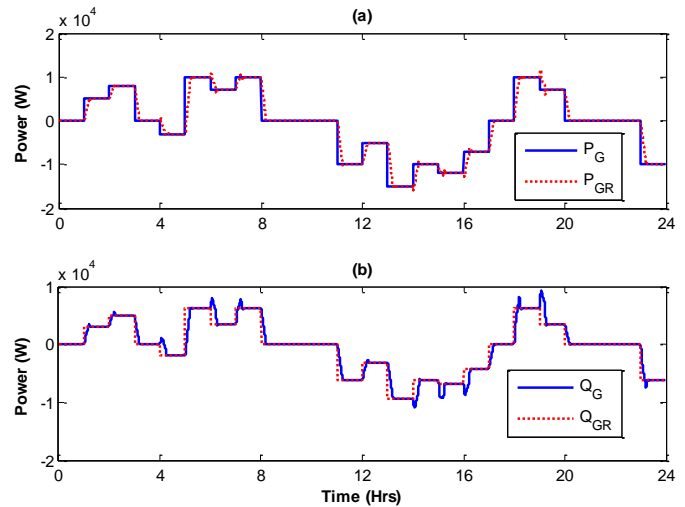


Figure 14: Utility grid power (a) Real power (b) Reactive power

PV System Results

Figure 15 shows the actual output and the reference power of PV system. As stated earlier, the PV array rating is 260 kW, so, the maximum output power is 252 kW. During a summer day, the sun rises at 5 H, but sun shines start at 5:30 H. Similarly, the sun sets at 7:50 H while sun rays disappears at 7:30 H which is clearly revealed from the above figure 15. The next major fact about the above figure is maximum power extraction. The incremental conductance based MPPT algorithm is controlled by PI controller. The dotted line represents the maximum power for each temperature and irradiance level, whereas the solid line represents the actual output power produced by PV using PI controlled based boost converter. At 12 H, the PV output power is at maximum of 252 kW on 1050 W/m^2 irradiance and 40°C temperature.

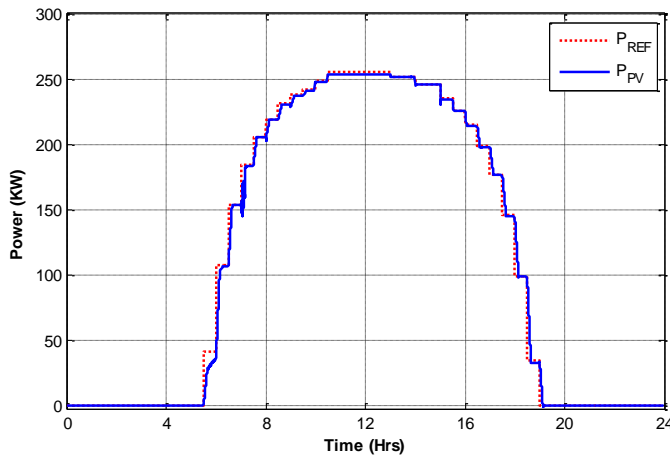


Figure 15: PV system output power

Main Inverter Results

The real and reactive power flowing through inverter is shown in figure 16. The power flowing through inverter is the difference of load demand minus grid power. Actually, the PV/SC/battery HRPS first provide its maximum available power, after that the grid will supply the remaining power. In this figure 16, the reference is shown in dotted line while the actual power is shown with solid. From figure 16, it is revealed that the slight overshoots and undershoots are due to dynamic response of PI controllers.

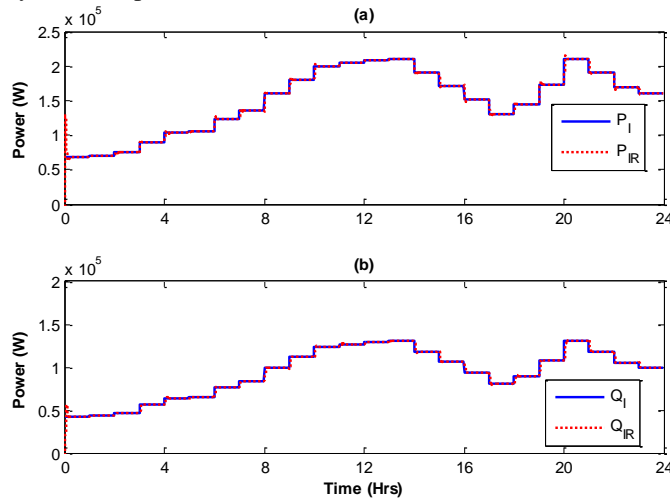


Figure 16: Power flow via main inverter (a) Real power (b) Reactive power

SC/Battery System

Figure 17 shows the SOCs and corresponding power of the battery and SC. From the figure, at $t=0$ to 7 H, the backup system i.e., SC and battery provides their maximum power. The battery provides 50 kW of power while the SC output power changes according to the demand and ranging from 0 to 60 kW. Similarly, on the other side, the SOCs of battery and SC changes accordingly. Battery and SC SOCs decreases to 48% and 72%, respectively. At $t = 8$ to 19 H, the PV output power is greater than load demand, so, the battery and SC starts charging. The negative power in figure 17(b) represents that SC and battery are charging. The battery gets

fully charged at 14 H and its power is zero while SC is charged up to 88%. After 19 H, the evening starts and PV power become zero, so, SC and battery delivers its available power and their SOCs decrease accordingly.

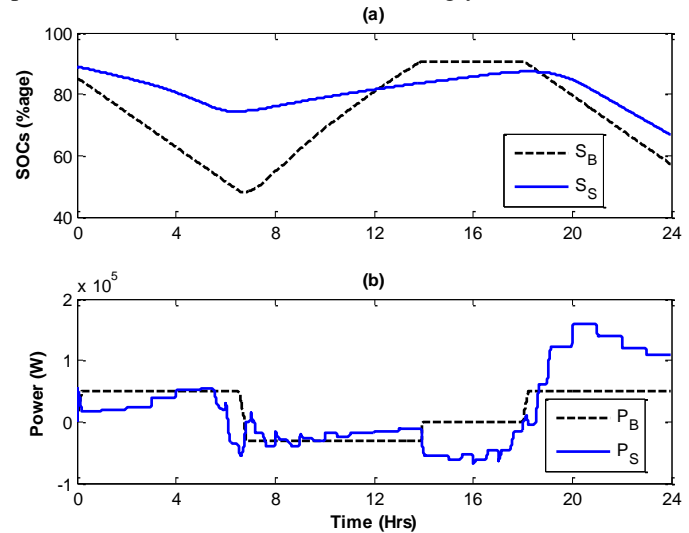


Figure 17: Battery/SC parameters (a) SOCs (b) Output power

Cumulative Results

Figure 18 shows plots of all powers. Starting from $t=0$ to 1 H, the load demand is 67 kW, so battery delivers its maximum power of 50 kW while the remaining 17 kW is provided by SC. For $t=1$ to 3 H, the load demand varies from 75 kW to 83 kW. In the same intervals, the grid is at the off peak load hour, so it delivers 5 kW to 8 kW of power, whereas battery and SC also plays its role by delivering 50 kW and 23 kW powers, respectively. For $t=3$ to 4 H, the grid is disconnected and 90 kW of load demand is satisfied with battery (50 kW) and SC (40 kW). For $t=4$ to 5 H, a load of 100 kW is applied on HRPS and the utility grid also needs a power of 3 kW. Therefore, cumulative load demand of residential load and grid load is shared between battery and SC by providing 50 kW and 53 kW of power, respectively. Till now PV does not play any role in satisfying load demand. For $t=5$ to 6 H, the load of 115 kW is applied. At $t=5.5$ H, the PV starts generating output power. In this time interval approximately 35 kW of power is provided by PV, whereas battery and SC shares 50 kW and 25 kW, respectively, but still the output power of PV is less than the load demand. For $t=6$ to 7 H, the load demand of 130 kW is applied. This is the most critical time duration, in which up to 6.5 H, the PV generates 115 kW of power less than the demand, and battery share 50 kW. After 6.5 H, the PV generates 153 kW of power greater than the load demand and there is no need of battery and SC, therefore, they start charging and their powers becomes negative as shown in the figure 18. For $t=7$ to 11 H, the load demand varies from 145 kW to 200 kW, whereas a grid is disconnected for the most of the time. The PV output power varies from 186 kW to 253 kW greater than the load demand. Similarly, on the other side the battery and SC are charging with 30 kW and 40 kW of powers, respectively.

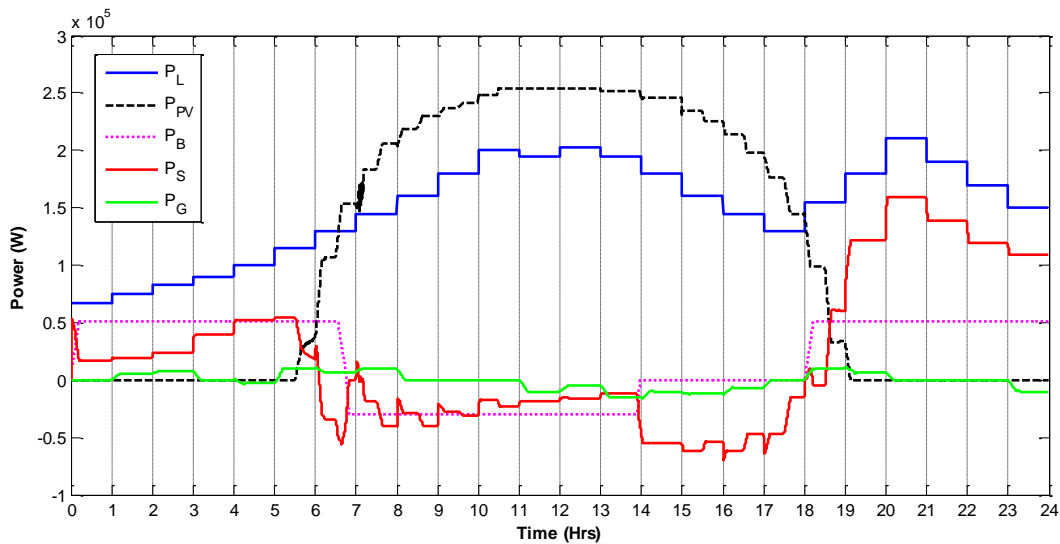


Figure 18: Output power of different energy sources/loads

For $t=11$ to 14 H, the load demand varies between 195 kW and 203 kW. It's a peak load hour, thus the grid also acts as a load in this duration and take power from HRPS ranging from 5 kW to 15 kW. A like previous case, the PV is generating power more than the load demand, SC and battery are charged from the surplus power generated by PV. For $t=14$ to 18 H, its afternoon timing and the output power of PV starts gradually decreasing (245 kW to 145 kW), but still greater than the load demand (180 kW to 130 kW). On the other side the battery is fully charged, so its power consumption is zero, whereas SC is still charged with maximum power of 66 kW and also grid takes maximum 12 kW of power. For $t=8$ to 9 H, the PV output power decreases and become zero while the battery and SC start discharging again. For $t=19$ to 24 , there is another load peak. The residential load varies between 150 kW and 210 kW, where the grid is disconnected for the majority of the time due to peak load hours. The battery shares its maximum 50 kW of power and the remaining power is efficiently provided by SC only

Stability Analysis

According to IEEE standards [24], the allowable limits for bus voltage is $\pm 5\%$. So for 700 V DC bus, the allowable limits are $\pm 35V$ of 700 V i.e., 665 V and 735 V. From figure 19, it is clearly revealed that the DC bus voltage is inside 665 V and 735V. The variation in DC bus is due to change in load. Usually, these changes occur at every hour.

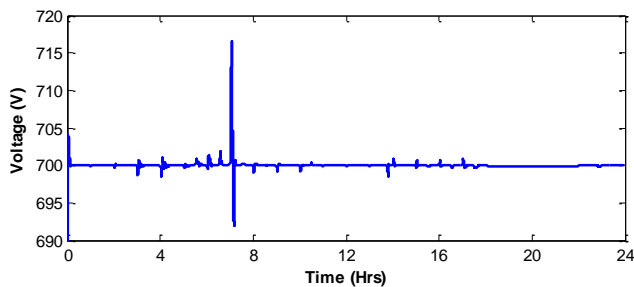


Figure 19: DC bus voltage

A system is called to be a stable system when power inside any system should be zero i.e., generated power must be

equal to the power consumption. From figure 20, it is clearly revealed that the net power inside the system is less than 1 W (which is negligible). So, the proposed system is called as stable system.

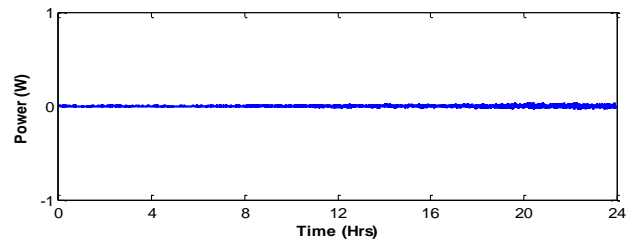


Figure 20: Net power on AC bus

For this system the fundamental load voltage and frequency are 440 V and 50 Hz, respectively. The acceptable values according to IEEE standards are $\pm 5\%$ for voltage and $\pm 0.8\%$ for frequency. So, their ranges are calculated as 418 V and 462 V for load voltage while 50.4 Hz and 49.6 Hz for load frequency. From figure 21, the load voltage and the frequency are in the acceptable limits.

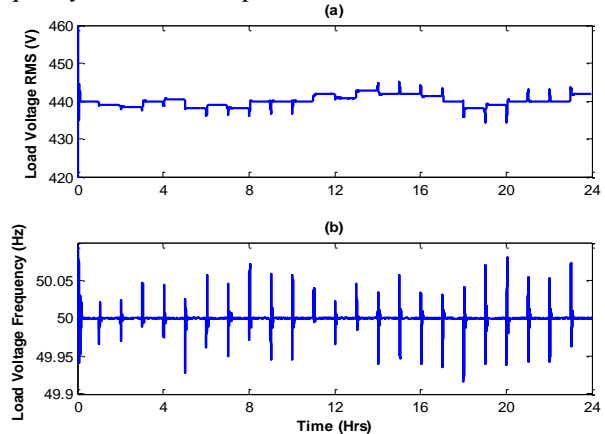


Figure 21: Load parameters (a) Voltage (b) Frequency

As stated earlier the load voltage RMS and frequency should be in $\pm 5\%$ and $\pm 0.8\%$. The time vs percent change plots of load voltage RMS and frequency are shown in figure 22. Whereas on the other side, the THD in a load voltage should be less than 5%. From figure 22, it is revealed that the THD is also in its acceptable limits.

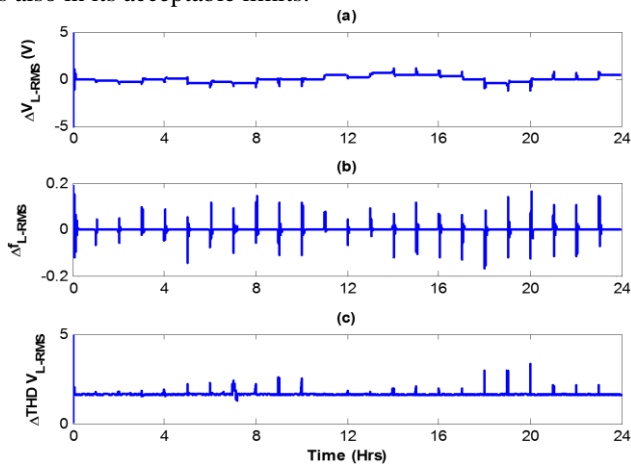


Figure 22: Power quality parameters (a) % change in load voltage RMS (b) % change in load voltage frequency (c) THD of load voltage

CONCLUSION

The PV/SC/battery hybrid system is developed for grid-off and grid-on residential applications with proper simple energy management strategy. The detailed modeling of system components, their integration, and control along with the utility grid is provided. The PV system has controlled by an incremental conductance based MPPT method followed by PI controllers. The performance of the system is tested under different weather patterns and load conditions for the simulation of one complete day. The proposed system exhibits excellent performance in terms of stability, voltage regulation and power quality. All the system components are developed in Matlab/Simulink.

ACKNOWLEDGMENT

The research work is supported by National Natural Science Foundation of China (No.51377184), International Science & Technology Cooperation Program of China (No.2013DFG61520) and Fundamental Research Funds for the Central Universities (No.CDJZR12150074).

REFERENCES

- [1] Hassan, S. Z. Mumtaz, S., Kamal, T. and Khan, L., "Performance of grid-integrated photovoltaic/fuel cell/electrolyzer/battery hybrid power system," *Power Generation System and Renewable Energy Technologies (PGSRET), 2015*: 1-8(2015).
- [2] Uzunoglu, M., Onar, O. and Alam, M., "Modeling, control and simulation of a PV/FC/UC based hybrid power generation system for stand-alone applications," *Renewable Energy*, **34**:509-520(2009).
- [3] Onar, O., Uzunoglu, M. and Alam, M., "Dynamic modeling, design and simulation of a wind/fuel cell/ultra-capacitor-based hybrid power generation system," *Journal of Power Sources*, **161**: 707-722(2006).
- [4] Hassan, S.Z., Li, H., Kamal, T. and Awais, M., "Stand-alone/grid-tied wind power system with battery/supercapacitor hybrid energy storage," *2015 International Conference on Emerging Technologies (ICET)*:1-6 (2015).
- [5] Kamal, T., Hassan, S.Z., Li, H. and Awais, M., "Design and power control of fuel cell/electrolyzer/microturbine/ultra-capacitor hybrid power plant," *International Conference on Emerging Technologies (ICET)*:1-6 (2015).
- [6] Mahmood, H., Michaelson, D. and Jiang, J., "Control strategy for a standalone PV/battery hybrid system," *IECON 2012-38th Annual Conference on IEEE Industrial Electronics Society*: 3412-3418 (2012).
- [7] Islam, S. and Belmans, R., "Grid independent photovoltaic fuel-cell hybrid system: design and control strategy," *KIEE International Transactions on Electrical Machinery and Energy Conversion Systems*, **5**: 399-405(2005).
- [8] Wu, Z., Tazvinga, H. and Xia, X., "Demand side management of photovoltaic-battery hybrid system," *Applied Energy*, **148**: 294-304(2015)
- [9] Glavin, M., Chan, P.K., Armstrong, S. and Hurley, W., "A stand-alone photovoltaic supercapacitor battery hybrid energy storage system," in *Power Electronics and Motion Control Conference*: 1688-1695(2008).
- [10] Logerais, P.O., Riou, O., Camara, M. A. and Durastanti, J. F., "Study of Photovoltaic Energy Storage by Supercapacitors through Both Experimental and Modelling Approaches," *Journal of Solar Energy*: **2013**, (2013).
- [11] Kollimalla, K. S., Mishra, M. K., and Narasamma, N. L., "Coordinated control and energy management of hybrid energy storage system in PV system," *International Conference on Computation of Power, Energy, Information and Communication (ICCPEIC)*: 363-368(2014).
- [12] Mao, M., Liu, Y., Jin, P., Huang, H., and Chang, L., "Energy coordinated control of hybrid battery-supercapacitor storage system in a microgrid," *4th IEEE International Symposium on Power Electronics for Distributed Generation Systems (PEDG)*:1-6 (2013).
- [13] Fahmi, M., Rajkumar, R. K., Arehli, R. and Isa, D., "Study on the effect of supercapacitors in solar PV system for rural application in Malaysia," *50th International Universities Power Engineering Conference (UPEC)*: 1-5 (2015).
- [14] Kamal, T., Hassan, S. Z., Khan, L. and Mumtaz, S., "Energy management and control of grid-connected wind/fuel cell/battery hybrid renewable energy system," *IEEE International Conference on Intelligent Systems Engineering (ICISE 2016)*: 1-6 (2016).
- [15] Espinosa-Trujillo, M., Flota-Bañuelos, M., Pacheco-Catalán, D., Smit, M. and Verde-Gómez, Y., "A novel stand-alone mobile photovoltaic/wind turbine/ultracapacitor/battery bank hybrid power system," *Journal of Renewable and Sustainable Energy*, **7**(2): 023125(2015).
- [16] El-Shater, T. F., Eskander, M. N. and El-Hagry, M. T., "Energy flow and management of a hybrid

- wind/PV/fuel cell generation system," *Energy Conversion and Management*, **47**(9-10): 1264-1280(2006).
- [17] Hannan, A. and Hasan, K. M., "ABC algorithm based scheduling and control of renewable hybrid power system," *Science International*, **27**(2): 1069-1074(2015).
- [18] Ali, A., Amjad, M., Mehmood, A., Asim, U. and Abid, A., "Cost effective power generation using renewable energy based hybrid system for Chakwal, Pakistan," *Science International* **27**(6): 6017-6022(2015).
- [19] Josephs, R., *Solar cell array design handbook*: NASA: (1976).
- [20] Rodrigues, E., Melício, R., Mendes, V. and Catalão, J., "Simulation of a solar cell considering single-diode equivalent circuit model," *International conference on renewable energies and power quality, Spain*: 13-15(2011).
- [21] Kamarzaman, A. N., and Tan, C. W., "A comprehensive review of maximum power point tracking algorithms for photovoltaic systems," *Renewable and Sustainable Energy Reviews*, **37**: 585-598(2014).
- [22] Hajizadeh, A. and Golkar, M. A., "Intelligent power management strategy of hybrid distributed generation system," *International Journal of Electrical Power & Energy Systems*, **29**: 783-795(2007).
- [23] Spyker, R. L., and Nelms, R. M., "Analysis of double-layer capacitors supplying constant power loads," *IEEE Transactions on Aerospace and Electronic Systems*, **36**: 1439-1443(2000).
- [24] "IEEE Standard for Interconnecting Distributed Resources with Electric Power Systems," *IEEE Std 1547-2003*: 1-28(2003).